

---

# High early strength calcium phosphate bone cement: Effects of dicalcium phosphate dihydrate and absorbable fibers

---

Elena F. Burguera,<sup>1</sup> Hockin H. K. Xu,<sup>2</sup> Shozo Takagi,<sup>2</sup> Laurence C. Chow<sup>2</sup>

<sup>1</sup>Instituto de Cerámica de Galicia, Universidad de Santiago de Compostela, 15782 Santiago de Compostela, Spain

<sup>2</sup>Paffenbarger Research Center, American Dental Association Foundation, National Institute of Standards and Technology, Gaithersburg, Maryland 20899

Received 15 November 2004; revised 8 June 2005; accepted 9 June 2005

Published online 25 August 2005 in Wiley InterScience (www.interscience.wiley.com). DOI: 10.1002/jbm.a.30497

**Abstract:** Calcium phosphate cement (CPC) sets *in situ* to form resorbable hydroxyapatite with chemical and crystallographic similarity to the apatite in human bones, hence it is highly promising for clinical applications. The objective of the present study was to develop a CPC that is fast setting and has high strength in the early stages of implantation. Two approaches were combined to impart high early strength to the cement: the use of dicalcium phosphate dihydrate with a high solubility (which formed the cement CPC<sub>D</sub>) instead of anhydrous dicalcium phosphate (which formed the conventional cement CPC<sub>A</sub>), and the incorporation of absorbable fibers. A 2 × 8 design was tested with two materials (CPC<sub>A</sub> and CPC<sub>D</sub>) and eight levels of cement reaction time: 15 min, 30 min, 1 h, 1.5 h, 2 h, 4 h, 8 h, and 24 h. An absorbable suture fiber was incorporated into cements at 25% volume fraction. The Gilmore needle method measured a hardening time of 15.8 min for CPC<sub>D</sub>, five-fold faster than 81.5 min for CPC<sub>A</sub>, at a powder:liquid ratio of 3:1. Scanning electron microscopy revealed the formation of nanosized rod-like hydroxyapatite crystals and platelet crys-

tals in the cements. At 30 min, the flexural strength (mean ± standard deviation; *n* = 5) was 0 MPa for CPC<sub>A</sub> (the paste did not set), (4.2 ± 0.3) MPa for CPC<sub>D</sub>, and (10.7 ± 2.4) MPa for CPC<sub>D</sub>-fiber specimens, significantly different from each other (Tukey's at 0.95). The work of fracture (toughness) was increased by two orders of magnitude for the CPC<sub>D</sub>-fiber cement. The high early strength matched the reported strength for cancellous bone and sintered porous hydroxyapatite implants. The composite strength  $S_c$  was correlated to the matrix strength  $S_m$ :  $S_c = 2.16S_m$ . In summary, substantial early strength was imparted to a moldable, self-hardening and resorbable hydroxyapatite via two synergistic approaches: dicalcium phosphate dihydrate, and absorbable fibers. The new fast-setting and strong cement may help prevent catastrophic fracture or disintegration in moderate stress-bearing bone repairs. © 2005 Wiley Periodicals, Inc. *J Biomed Mater Res* 75A: 966–975, 2005

**Key words:** calcium phosphate cement; hydroxyapatite; early strength; fast setting; absorbable fibers; bone repair

---

## INTRODUCTION

Calcium phosphate cements can be molded and self-harden in the prepared bone site to form resorbable hydroxyapatite.<sup>1</sup> The first self-setting calcium phosphate cement, referred to as CPC, was developed

Certain commercial materials and equipment are identified in this article to specify experimental procedures. In no instance does such identification imply recommendation by NIST or the ADA Foundation, or that the material identified is necessarily the best available for the purpose.

Correspondence to: H. Xu; e-mail: hockin.xu@nist.gov

Contract grant sponsor: USPHS; contract grant numbers: R29 DE12476, R01 DE14190, R01 DE11789

Contract grant sponsor: NIST

Contract grant sponsor: ADAF

Contract grant sponsor: Great-West Life Annuity

in 1986.<sup>1</sup> Since then, many compositions of calcium phosphate cements have been formulated and tested.<sup>2–6</sup> CPC is comprised of a mixture of fine particles of tetracalcium phosphate [TTCP: Ca<sub>4</sub>(PO<sub>4</sub>)<sub>2</sub>O] and dicalcium phosphate anhydrous [DCPA: CaHPO<sub>4</sub>].<sup>1</sup> Because the hydroxyapatite from CPC is formed in an aqueous environment at body temperature, it is more similar to biological apatites than sintered hydroxyapatite formed at high temperatures.<sup>7–11</sup> Due to its self-setting ability, excellent osteoconductivity, and bone replacement capability, CPC is highly promising for a wide range of clinical applications.<sup>7–11</sup>

However, the low strength of CPC has limited its use to only nonstress applications,<sup>8</sup> and clinical usage has been severely hindered by its brittleness.<sup>10</sup> One clinical study on the repair of periodontal bone defects demonstrated that the brittle nature of CPC caused early exfoliation of all or pieces of the implant.<sup>12</sup> An-

other major shortcoming is that it takes a relatively long time for the CPC paste to set. A long setting time can result in the crumbling of CPC when the paste comes in contact with physiological fluids, or if bleeding occurs due to the difficulty in some cases to achieve complete hemostasis.<sup>4,13,14</sup> Low strength in the early postoperative stage (low early strength) can result in the cement to fail or disintegrate under even moderate stresses. Studies were carried out to overcome these disadvantages of CPC.<sup>14–17</sup> Hydroxypropyl methylcellulose and other gelling agents were incorporated into CPC to render the paste more cohesive and resistant to washout.<sup>14,15</sup> Chitosan, a biopolymer, imparted nonrigidity, high toughness, and fast-setting to CPC.<sup>16,17</sup> In a more recent study,<sup>18</sup> dicalcium phosphate dihydrate (DCPD,  $\text{CaHPO}_4 \cdot 2\text{H}_2\text{O}$ ), a calcium phosphate compound known to possess a relatively high solubility and resorbability,<sup>19,20</sup> was used to replace the DCPA component in CPC. The high solubility of DCPD resulted in the fast setting of the cement, yielding a hardening time of about 15 min with water used as the cement liquid and 6 min with the use of a phosphate solution, although the phosphate solution resulted in a lower cement strength.<sup>18</sup>

The objective of the present study was to develop a hydroxyapatite cement that can quickly develop high strength shortly after paste placement. Two approaches were tested: the use of DCPD in the place of DCPA to form the cement, and the incorporation of absorbable fibers. The fibers would provide the needed early strength and then be dissolved to create long cylindrical macropores for cell infiltration and bone ingrowth. It was hypothesized that combining the two approaches synergistically would substantially increase the early strength, elastic modulus, and work of fracture (toughness) for the cement compared to using a single approach. It was further hypothesized that these properties would significantly depend on the cement reaction time (or incubation time).

## MATERIALS AND METHODS

### Preparation of $\text{CPC}_A$ and $\text{CPC}_D$

The tetracalcium phosphate (TTCP) powder was synthesized from a solid-state reaction between  $\text{CaHPO}_4$  (dicalcium phosphate anhydrous, DCPA) and  $\text{CaCO}_3$  (Baker Analyzed Reagents, J. T. Baker Chemical, Phillipsburg, NJ), which were mixed and heated at 1500°C for 6 h in a furnace (Model 51333, Lindberg, Watertown, WI). The heated mixture was quenched to room temperature, ground, and sieved to obtain TTCP particles with sizes ranging from about 1 to 60  $\mu\text{m}$ , with a median particle size of 20  $\mu\text{m}$ . The DCPA powder was ground in 95% ethanol for 24 h to obtain

particles with sizes ranging from 0.4  $\mu\text{m}$  to 6  $\mu\text{m}$ , with a median particle size of 1.2  $\mu\text{m}$ . The TTCP and DCPA powders were then mixed in a micromill (Bel-Alert Products, Pequannock, NJ) in equimolar amounts to form the powder for the cement designated as  $\text{CPC}_A$ .

Preliminary studies using commercial dicalcium phosphate dihydrate (DCPD) powders yielded long setting times of greater than 1 h for the TTCP-DCPD paste, likely due to certain unidentified impurities in the commercial powders.<sup>18</sup> Therefore, the DCPD powder used in the present study was prepared in the laboratory. The pH was slowly raised via the addition of  $\text{CaCO}_3$  for a DCPD–monocalcium phosphate monohydrate singular point solution at a pH of 1.9 and a temperature of 4°C. DCPD that precipitated before the pH reached about 3.5, which is significantly below the hydroxyapatite-DCPD singular point of 4.2, was collected to avoid possible contamination of the DCPD by hydroxyapatite. The DCPD was washed, first with distilled water, and then with ethanol of 95%, and then dried in air. The DCPD was ground in water with a ball mill to obtain particles with size ranging from approximately 0.5 to 4  $\mu\text{m}$  and a median particle size of 1.3  $\mu\text{m}$ . The DCPD powder was mixed with the TTCP powder at a molar ratio of 1:1 to form the powder for the cement referred to as  $\text{CPC}_D$ .

### Measurement of cement setting time

The CPC powder and liquid were manually mixed with a spatula to form a paste that was filled into a stainless steel mold of 6-mm diameter and 3-mm depth.<sup>21</sup> Distilled water was used as the cement liquid. Each specimen in the mold was sandwiched between two glass slides, and the assembly was incubated in a humidior with 100% relative humidity at 37°C. The hardening time was measured using the Gilmore needle method with a load of 453.5 g and a flat tip diameter of 1.06 mm.<sup>22</sup> A cement specimen was considered set when the needle loaded onto the specimen surface failed to leave a perceptible indentation. The time measured from the paste being mixed to this point was used as the setting time. A  $2 \times 5$  full-factorial design was tested with two materials ( $\text{CPC}_A$  and  $\text{CPC}_D$ ) and five powder:liquid mass ratios (4.5:1, 4:1, 3.5:1, 3:1, and 2.5:1).

### Fabrication of $\text{CPC}_A$ and $\text{CPC}_D$ specimens

To investigate the early strength of CPC and its dependence on cement incubation time, a  $2 \times 8$  full-factorial design was tested with two materials ( $\text{CPC}_A$  and  $\text{CPC}_D$ ) and eight levels of incubation time: 15 min, 30 min, 1 h, 1.5 h, 2 h, 4 h, 8 h, and 24 h. The incubation time was defined as the time from the paste being mixed to the specimen being tested in three-point flexure. An intermediate powder:liquid mass ratio of 3:1 was selected because the paste was relatively flowable and cohesive. The paste at 4.5:1 was quite dry, and that at 2.5:1 resulted in a lower strength for the set cement. The CPC powder and water were mixed with a spatula to form a paste that was filled into a stainless steel mold of  $3 \times 4 \times 25$  mm. The paste in each mold was

sandwiched between two glass slides, and set in a humidior with 100% relative humidity at 37°C. For incubation times of 4 h or less, the specimen was demolded and tested in flexure as described in the following section. For incubation times of greater than 4 h, the specimen was demolded at 4 h, then immersed in distilled water in the humidior for the remainder of the prescribed incubation time.

### Mechanical testing

A three-point flexural test with a span of 20 mm was used to fracture the specimens at a crosshead speed of 1 mm/min on a computer-controlled universal testing machine (model 5500R, Instron, Canton, MA). Flexural strength, elastic modulus, and work of fracture were measured.

### Conversion to hydroxyapatite

Powder X-ray diffraction (XRD) analysis was used to examine the CPC conversion to hydroxyapatite.<sup>17,23</sup> The halves from the flexural specimens were dried and milled into a powder by mortar and pestle to characterize the hydroxyapatite formation for CPC<sub>A</sub> and CPC<sub>D</sub>. The XRD patterns were recorded with a powder X-ray diffractometer (Rigaku, Danvers, MA) with the use of graphite-monochromatized copper K<sub>α</sub> radiation ( $\lambda = 0.154$  nm) generated at 40 kV and 40 mA. The 002 peak intensity of hydroxyapatite was used to measure the percentage of conversion to hydroxyapatite. All data were collected in a continuous scan mode ( $1^\circ 2\theta \text{ min}^{-1}$ , step time 0.6 s, step size  $0.01^\circ$ ).

### Fiber reinforcement

An absorbable suture fiber (Vicryl polyglactin 910, Ethicon, Somerville, NJ) was used. This suture consisted of individual fibers braided into a bundle with a bundle diameter of about 322  $\mu\text{m}$  that provided substantial strength and toughness for about 4 weeks, and then dissolved and produced macropores in CPC as shown in a previous study.<sup>24</sup> As in the previous study, the suture was cut to filaments 8 mm in length. The CPC powder was mixed with distilled water at a powder:liquid mass ratio of 3:1. The filaments were mixed with the CPC paste randomly to form a composite paste, which was placed into the  $3 \times 4 \times 25$  mm molds and set in the humidior. During three-point flexural testing, most of the fiber-reinforced specimens were still intact after the matrix had cracked, due to fibers bridging the cracks. The test was stopped at a displacement of 2.0 mm for a consistent calculation of work of fracture.<sup>25</sup>

### Microscopy and statistics

The fracture surfaces of specimens at various incubation times were sputter coated with gold and examined with a

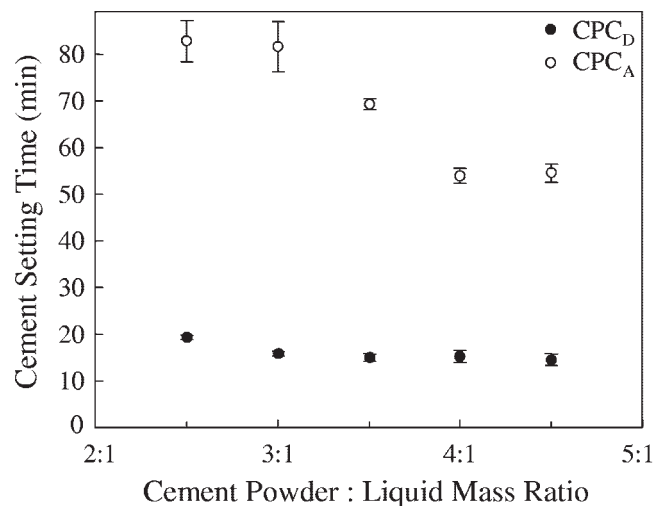


**Figure 1.** Cement setting time versus powder:water ratio. Each value is the mean of four measurements with the error bar showing one standard deviation (mean  $\pm$  standard deviation;  $n = 4$ ). CPC<sub>D</sub>, using dicalcium phosphate dihydrate, was much faster setting than the conventional cement CPC<sub>A</sub>, with anhydrous dicalcium phosphate.

scanning electron microscope (SEM, JEOL 5300, Peabody, MA). Two-way and one-way analysis of variance (ANOVA) was performed to detect significant effects. Tukey's multiple comparison was used to compare the data at a family confidence coefficient of 0.95. One standard deviation was used as the estimated standard uncertainty of the measurements. These values should not be compared with data obtained in other laboratories under different conditions.

## RESULTS

### Setting time

Figure 1 shows the cement setting time as a function of powder:liquid ratio. Each value is the mean of four measurements, with the error bar showing one standard deviation (mean  $\pm$  standard deviation;  $n = 4$ ). Two-way ANOVA identified significant effects ( $p < 0.001$ ) of powder:liquid ratio and cement composition. CPC<sub>A</sub> had a setting time ranging from  $82.8 \pm 4.4$  min to  $54.5 \pm 1.9$  min. The setting time for CPC<sub>D</sub> was much shorter, ranging from  $19.3 \pm 0.5$  min to  $14.5 \pm 1.3$  min. At a powder:liquid mass ratio of 3:1, the setting time was  $15.8 \pm 0.5$  min for CPC<sub>D</sub>, significantly faster than  $81.5 \pm 5.3$  min for CPC<sub>A</sub> (Tukey's multiple-comparison test; family confidence coefficient = 0.95).

### Mechanical properties

Figure 2 is a plot of the flexural strength, elastic modulus, and work of fracture for CPC<sub>A</sub> and CPC<sub>D</sub>

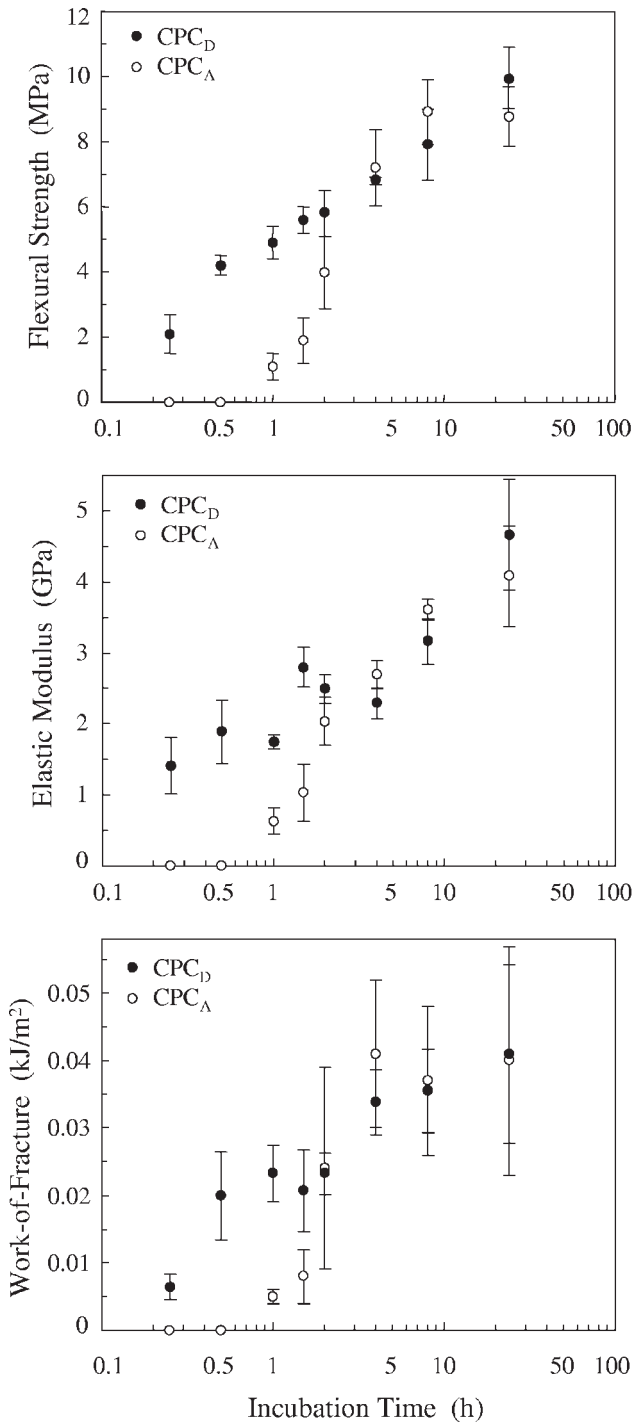


**Figure 2.** Flexural strength, elastic modulus, and work of fracture versus incubation time. Each value was the mean of five measurements, with the error bar showing one standard deviation (mean ± standard deviation;  $n = 5$ ). For both CPC<sub>D</sub> and CPC<sub>A</sub> mechanical properties increased with increasing incubation time. However, in the early stage after paste mixing, CPC<sub>D</sub> had much higher mechanical properties than CPC<sub>A</sub>. CPC<sub>A</sub> failed to set at incubation times up to 30 min. CPC<sub>D</sub> achieved high early properties (15 min to 2 h) without compromising later-stage properties from 2 to 24 h.

without fibers. Two-way ANOVA of the  $2 \times 8$  design showed significant effects of composition and incubation time, with a significant interaction between the two variables ( $p < 0.001$ ). For CPC<sub>A</sub>, the paste failed to set at incubation time up to 30 min. This was radically different from CPC<sub>D</sub>, which produced well-set, smooth, strong specimens. CPC<sub>D</sub> had flexural strengths (mean ± standard deviation;  $n = 5$ ) of  $2.1 \pm 0.6$  MPa and  $4.2 \pm 0.3$  MPa, at incubation times of 15 min and 30 min, respectively.

At 1 h, CPC<sub>A</sub> started to set, exhibiting a flexural strength of  $1.1 \pm 0.4$  MPa. It then monotonically increased to  $1.9 \pm 0.7$  MPa at 1.5 h and  $8.9 \pm 1.5$  MPa at 8 h, after which it plateaued. In comparison, CPC<sub>D</sub> possessed strengths of  $4.9 \pm 0.5$  MPa at 1 h and  $5.6 \pm 0.4$  MPa at 1.5 h, three–four times higher than their CPC<sub>A</sub> counterparts. The strengths of CPC<sub>A</sub> and CPC<sub>D</sub> became statistically similar after 2 h (Tukey’s at family confidence coefficient of 0.95). Similarly, the elastic modulus and work of fracture of CPC<sub>D</sub> were in general several times higher than those of CPC<sub>A</sub> at incubation times from 15 min to 1.5 h, then became statistically similar after 2 h.

**Conversion to hydroxyapatite**

XRD analysis showed that the conversion of the cement components to hydroxyapatite occurred for both CPC<sub>A</sub> and CPC<sub>D</sub>. The percentage (%) of CPC converted to hydroxyapatite is listed in Table I. From 1–2 h of incubation, a small amount of hydroxyapatite was formed in CPC<sub>A</sub>. A relatively large amount of hydroxyapatite was formed in CPC<sub>D</sub> as early as 15 min. After incubation time of 2 h, the hydroxyapatite formation accelerated in CPC<sub>A</sub> at a faster rate than in CPC<sub>D</sub>.

SEM micrographs of fracture surfaces of CPC<sub>D</sub> specimens are shown in Figure 3(A,B) at 15-min incubation time and in Figure 3(C,D) at 30-min incubation time.

**TABLE I**  
Percentage of CPC conversion to Hydroxyapatite (HA) as a Function of Incubation Time (Mean ± Standard Deviation;  $n = 3$ ) Obtained from Powder X-Ray Diffraction Analysis

Incubation Time (h)	% HA Conversion in CPC <sub>A</sub>	% HA Conversion in CPC <sub>D</sub>
0.25	Paste did not set	$13.4 \pm 0.0$
0.5	Paste did not set	$18.1 \pm 2.1$
1	$6.2 \pm 0.0$	$19.3 \pm 2.1$
1.5	$6.2 \pm 0.0$	$26.4 \pm 2.1$
2	$8.6 \pm 4.1$	$27.6 \pm 0.0$
4	$45.4 \pm 3.6$	$34.7 \pm 0.0$
8	$79.8 \pm 2.1$	$46.6 \pm 5.4$
24	$85.7 \pm 2.1$	$53.7 \pm 4.1$

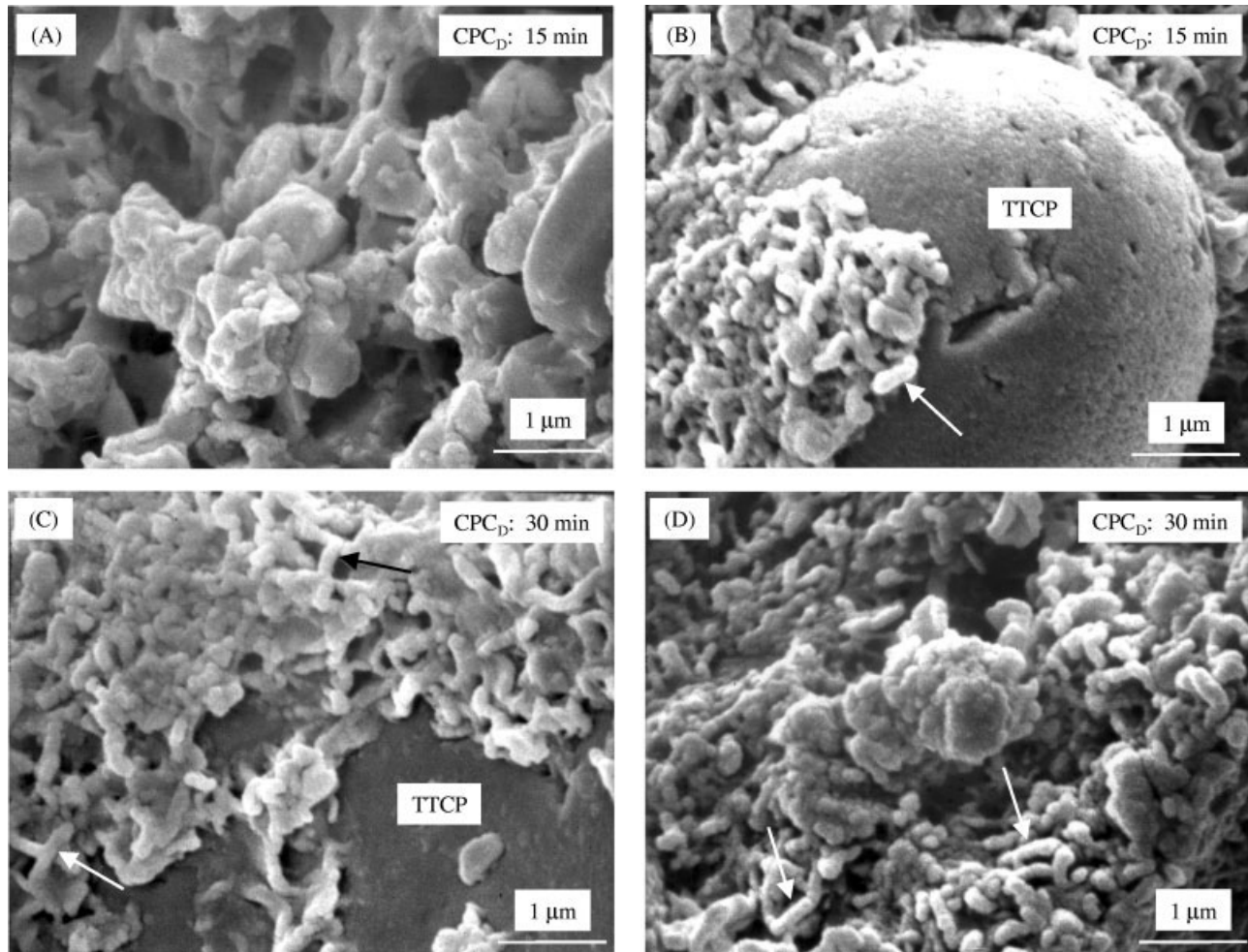


**Figure 3.** SEM at 15 and 30 min for  $CPC_D$ . (A) At 15 min, DCPD particles were still visible. These particles were similar to the starting DCPD particles with a median particle size of 1.3  $\mu\text{m}$ . (B) Small crystals formed on the surfaces of TTCP particles at 15 min. These small crystals are hydroxyapatite crystals because they were not present in the starting powder, and XRD detected the formation of hydroxyapatite. (C) At 30 min, some TTCP particles were covered with the elongated hydroxyapatite crystals, and (D) hydroxyapatite crystals were also observed away from TTCP.

$CPC_A$  is not shown here because it did not set. At 15 min [Fig. 3(A)], some areas of  $CPC_D$  consisted of DCPD particles that were not yet consumed in the setting reaction (earlier, the starting powder had a DCPD median particle size of 1.3  $\mu\text{m}$  and a TTCP median particle size of 17  $\mu\text{m}$ ). Other areas of the  $CPC_D$  fracture surfaces showed small crystals forming on the surfaces of TTCP particles [Fig. 3(B)]. These small, elongated crystals had a diameter of about 0.1  $\mu\text{m}$  and a length of 0.3–0.5  $\mu\text{m}$  [arrows in (B–D)]. They are believed to be hydroxyapatite crystals because they were not present in the starting powder, and XRD detected the formation of hydroxyapatite in these specimens. At 30 min, some TTCP particles were nearly entirely covered with the elongated hydroxyapatite crystals [arrows in Fig. 3(C)], and hydroxyapatite crystals were also observed away from the TTCP particles [arrows in Fig. 3(D)].

Figure 4 shows that at 1 h, hydroxyapatite crystals

were observed in both  $CPC_D$  and  $CPC_A$ . Some areas of the fracture surfaces of  $CPC_D$  showed a mixture of small crystals and platelet crystals [Fig. 4(A)]. Larger platelet crystals of a size of a few micrometers were occasionally observed in  $CPC_D$  [Fig. 4(B)]. Submicron, elongated crystals were observed in the fractured surfaces of  $CPC_A$  [Fig. 4(C)], but no platelets were observed. In addition, DCPD particles similar to Figure 3(A) and TTCP particles similar to Figure 3(B) were still observed, indicating that the setting reaction was ongoing.

At 24 h, submicron crystals were frequently observed in the fracture surfaces of  $CPC_D$ , as shown in Figure 5(A), whereas larger platelets were occasionally found [Fig. 5(B)]. The platelets had a wide dimension on the order of 2  $\mu\text{m}$  and a thickness of about 0.1  $\mu\text{m}$ .  $CPC_A$  consisted of numerous rod-like hydroxyapatite crystals with a diameter of about 0.1  $\mu\text{m}$  and a length of up to 0.5  $\mu\text{m}$  [Fig. 5(C)].

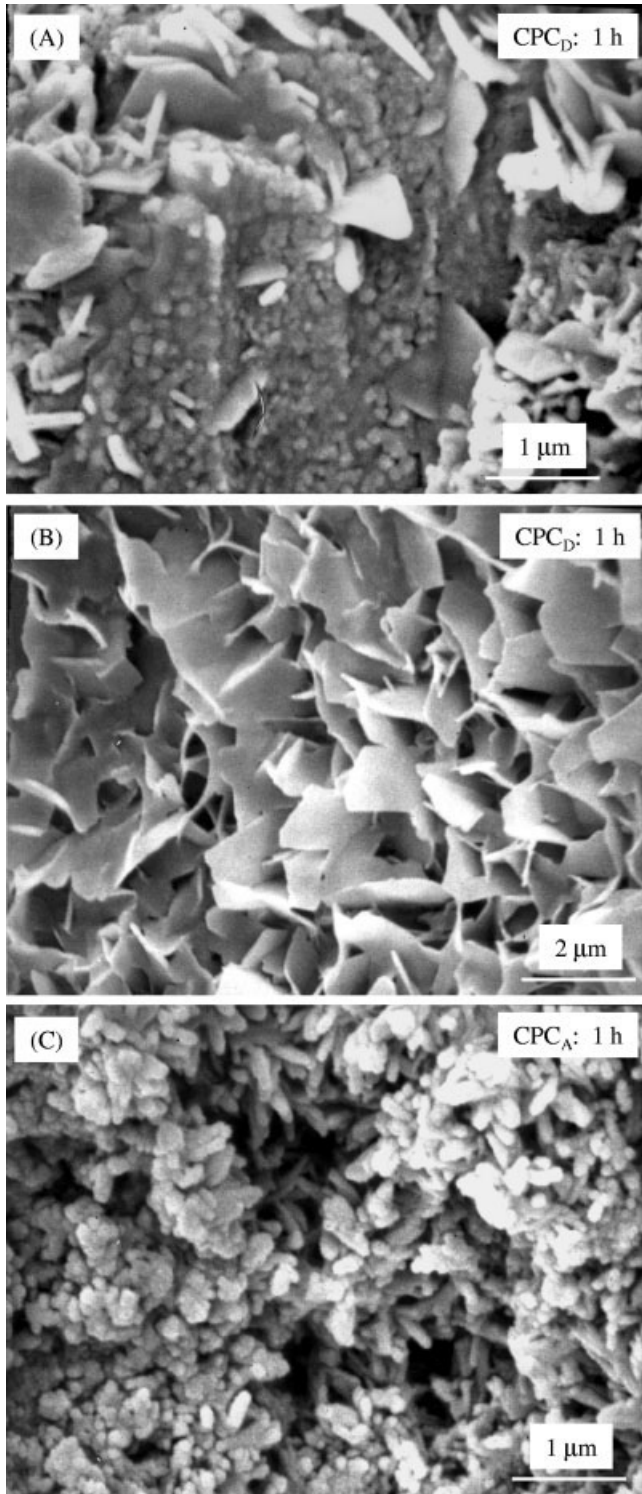


**Figure 4.** SEM at 1 h for (A) and (B) CPC<sub>D</sub> and (C) CPC<sub>A</sub>. (A) Some areas of the fractured surfaces of CPC<sub>D</sub> showed a mixture of small crystals and platelet crystals. (B) Larger platelet crystals were occasionally observed. (C) Small elongated crystals were observed in CPC<sub>A</sub>.

**Fiber reinforcement**

To further increase the early strength of the hydroxyapatite cements, absorbable fibers were incorpo-

rated into the pastes. Figure 6 shows flexural strength, elastic modulus, and work of fracture versus incubation time. Both CPC<sub>D</sub> and CPC<sub>A</sub> contained 25% volume fraction of fibers. At incubation times of 15 and 30

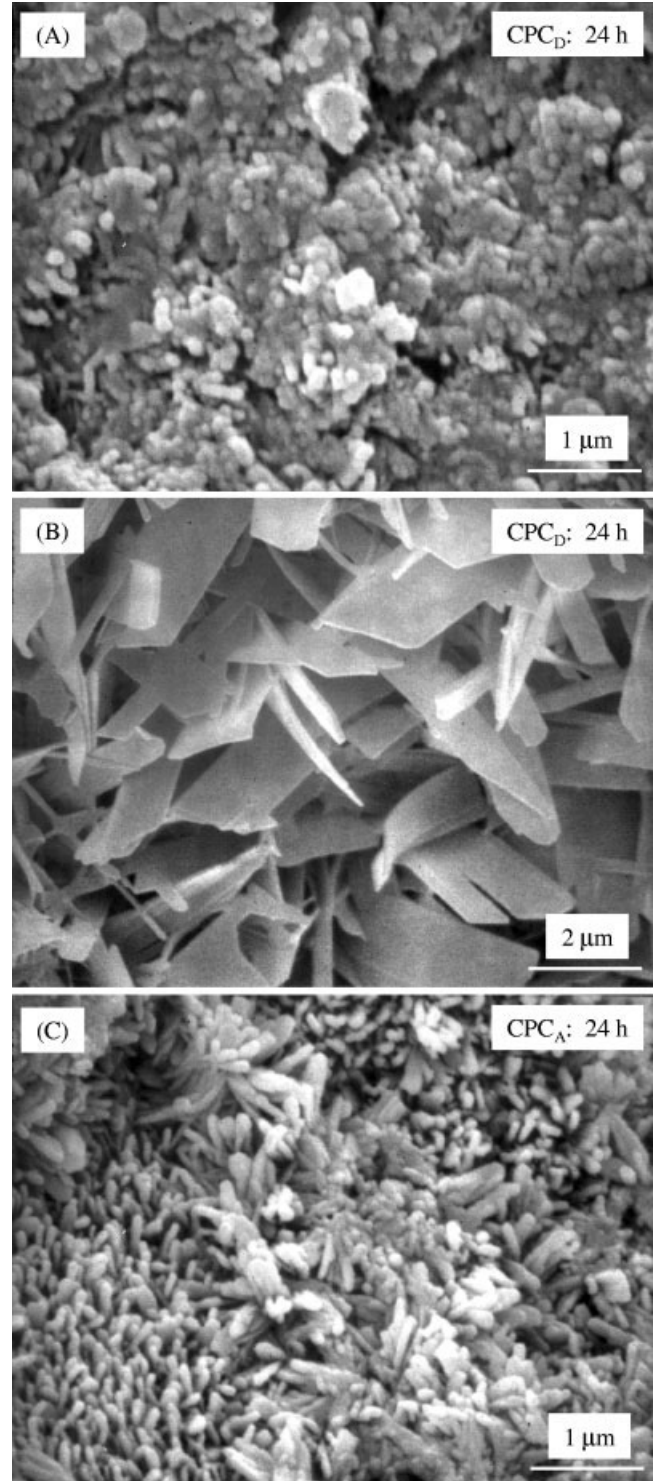


**Figure 5.** SEM at 24 h for (A) and (B) CPC<sub>D</sub> and (C) CPC<sub>A</sub>. (A) Small crystals were frequently observed in the fractured surfaces. (B) Large platelets were occasionally observed. (C) Rod-like hydroxyapatite crystals were observed in CPC<sub>A</sub>.

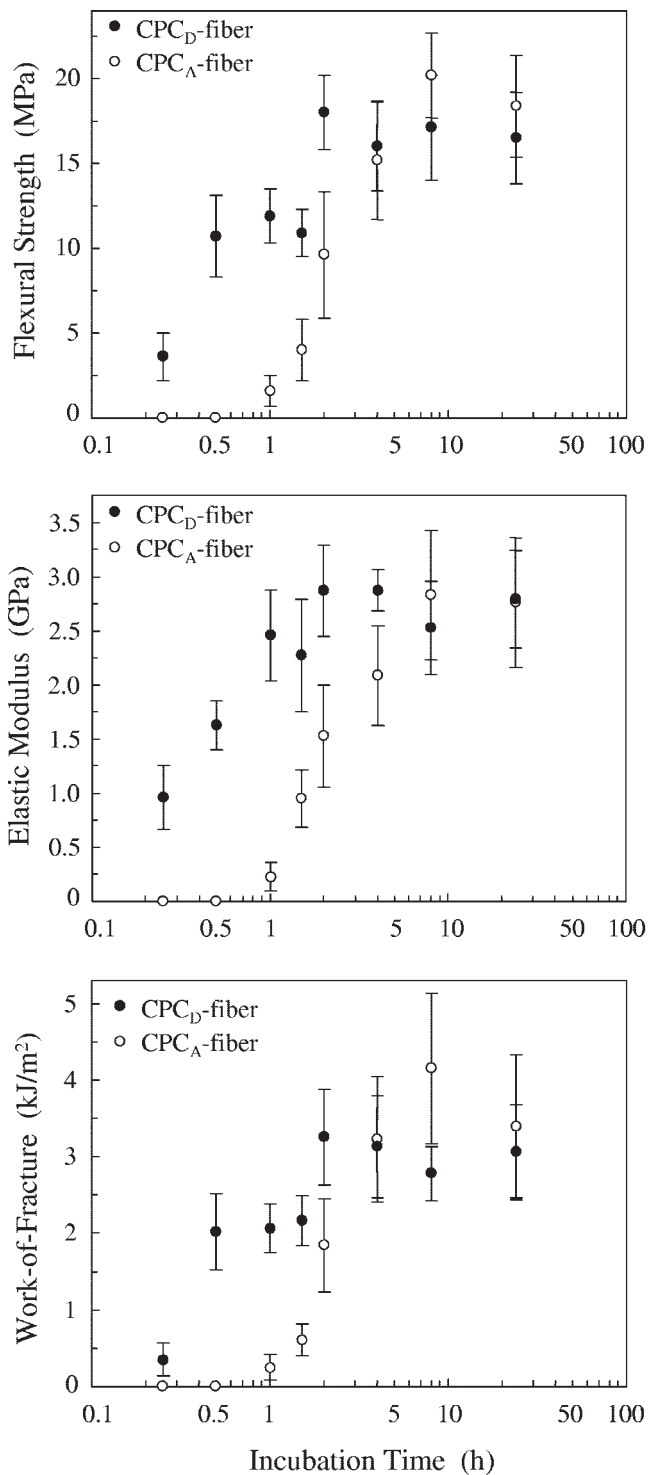


**Figure 6.** Fiber reinforcement. Flexural strength, elastic modulus, and work of fracture were higher for CPC<sub>D</sub> than for CPC<sub>A</sub> at incubation times of 15 min to 2 h. For both materials, properties first increased with incubation time, then started to plateau after 8 h. Compared to specimens without fibers (Fig. 2), the strengths of CPC<sub>D</sub> and CPC<sub>A</sub> fibers were generally about two times higher, the modulus values were slightly lower due to the fibers being less stiff than CPC, and the work of fracture was increased by two orders of magnitude because of fiber reinforcement. Each value was the mean of five measurements with the error bar showing one standard deviation (mean  $\pm$  standard deviation;  $n = 5$ ).

min, CPC<sub>D</sub>-fiber specimens had strengths (mean  $\pm$  standard deviation;  $n = 5$ ) of  $3.6 \pm 1.4$  MPa and  $10.7 \pm 2.4$  MPa, respectively, while CPC<sub>A</sub> failed to set. At 1 h, CPC<sub>D</sub>-fiber specimens reached a strength of  $11.9 \pm 1.6$  MPa, whereas that of CPC<sub>A</sub> fiber was only  $1.6 \pm 0.9$  MPa. For both materials, the strength, elastic modulus, and work of fracture first increased with incubation time, then plateaued after 8 h. Compared to specimens without fibers (Fig. 2), the strengths of CPC<sub>D</sub> and CPC<sub>A</sub> fibers were generally about two times higher, the modulus values were slightly lower due to the polymer fibers being less stiff than CPC, and the work of fracture was increased by two orders of magnitude because of fiber reinforcement.

## DISCUSSION

Hydroxyapatite cement with substantially improved early strength, elastic modulus, and toughness was developed in the present study via two approaches: (1) use of DCPD instead of DCPA in the cement, and (2) incorporation of absorbable fibers. The first approach resulted in a fast-setting cement, with hardening time reduced by a factor of four (Fig. 1). In the clinical situation, the surgeon needs to place a CPC paste into the prepared bone site and then wait for the paste to sufficiently harden before closing the wound. Otherwise the soft paste could be deformed easily to lose its geometrical shape by the stresses generated in closing the wound, or even be disintegrated and fail to set into a cohesive implant. A long setting time could cause problems because of the cement's inability to support stresses within this time period.<sup>14,26</sup> A severe inflammatory response was observed when CPC failed to set and disintegrated, likely due to a low initial mechanical strength.<sup>13</sup> Another study revealed a transient inflammatory response without foreign-body reaction.<sup>27</sup> The surgeon needs to touch or palpate the cement, or tap the cement lightly, to make sure that the cement has sufficiently set. Only after that can the surgeon close the wound by suturing together the muscle, fascia, and the skin. A hardening time of 15 min for CPC<sub>D</sub> (powder:liquid = 3:1) would save valuable time clinically, compared to 80 min for the conventional CPC<sub>A</sub>.

The TTCP-DCPD cement set faster than the TTCP-DCPA cement, possibly because the DCPD particles have a faster dissolution rate than DCPA.<sup>18–20</sup> The same faster dissolution of DCPD was likely responsible for the higher hydroxyapatite formation for CPC<sub>D</sub> than CPC<sub>A</sub> in the first 2 h of cement reaction (Table I). CPC<sub>A</sub> had a rapid increase in hydroxyapatite formation after 4 h. This was probably because once DCPA started to significantly dissolve, numerous DCPA particles started dissolving simultaneously. In examining

hydroxyapatite formation, the gold coating on the SEM specimen surfaces prevented charging, but it may have also had some influence on the sharpness of the edges of the hydroxyapatite crystals. This is because some hydroxyapatite crystals in several previous studies<sup>23,28</sup> appeared to have slightly sharper edges. Figures 3–5 showed the formation of hydroxyapatite crystals in CPC<sub>D</sub> as early as 15 min, consistent with its fast setting time, and the presence of platelets [Figs. 4(B) and 5(B)] in CPC<sub>D</sub> that were generally absent in CPC<sub>A</sub>. However, fast setting did not occur with the TTCP-DCPD cement in the pilot study, when commercial DCPD powders were used.<sup>18</sup> This was possibly due to unidentified impurities in the commercial powders.<sup>18</sup> Later, the DCPD powders were processed in the laboratory, as described in the Materials and Methods section, which resulted in much faster setting of the cement. Several previous studies developed novel cements based on DCPD that were self-setting and bioactive, and useful for orthopedic, dental, and drug-delivery applications.<sup>29–32</sup> Compared to the DCPD cements in the previous studies, the cement in the present study had a much shorter hardening time (15 min vs. > 1 h) and higher mechanical strength,<sup>18</sup> without the use of hydroxyapatite seeds. Although a higher purity of the DCPD in the present study may have contributed to the faster setting and higher strength, further studies are needed to examine other processing factors. Previous studies have reported a range of CPC setting times from about 20 min to more than 100 min,<sup>33</sup> suggesting the dependence of setting on microstructural and processing parameters. Hence it is possible that the setting time of both CPC<sub>D</sub> and CPC<sub>A</sub> could be further shortened by optimizing the particle size and size distribution, which warrants further study.

Early strength was dramatically increased via the two approaches. At 30 min after paste mixing, the conventional CPC (CPC<sub>A</sub>) was still a paste and had no measurable strength. The first approach resulted in the setting of solid CPC<sub>D</sub> specimens with a flexural strength 4.2 MPa. The second approach resulted in the CPC<sub>D</sub>-fiber specimens possessing an even higher strength of 10.7 MPa. In comparison, the flexural strength of available sintered porous hydroxyapatite implants ranged from 2–11 MPa.<sup>34</sup> Cancellous bone has a tensile strength of about 3.5 MPa.<sup>35</sup> The CPC<sub>D</sub>-fiber paste could harden in 15 min to develop a strength of 3.6 MPa, similar to that of cancellous bone. At 30 min after implantation, it further developed a strength similar to sintered porous hydroxyapatite implants. Sintered hydroxyapatite implants require machining to fit to a prepared bony defect, and are usually not resorbable or replaceable by new bone.<sup>36,37</sup> Histologic analyses showed that nonresorbable hydroxyapatite induced little new bone fill, and very limited, if any, periodontal bone regeneration.<sup>37</sup> In

contrast, the CPC<sub>D</sub>-fiber paste can harden *in situ* in the bone cavity, resulting in intimate contact with neighboring bone, and both CPC and the fiber can be resorbed and replaced by new bone. The elastic modulus of CPC<sub>D</sub>-fiber specimens reached 1.63 GPa at 30 min, compared to an elastic modulus measured in flexure of about 12.8 GPa for cortical bone<sup>38</sup> and 0.3 GPa for cancellous bone.<sup>39</sup> The work of fracture at 30 min for CPC<sub>D</sub> fiber was 2.0 kJ/m<sup>2</sup>, compared to a work of fracture of about 1.5 kJ/m<sup>2</sup> for cortical bone.<sup>40</sup> Such improvements in mechanical properties in the early stage immediately after paste placement, imparted by the two approaches, should help protect the CPC implant from catastrophic fracture or disintegration under stresses. Animal and clinical studies are needed to investigate the use of the CPC<sub>D</sub>-fiber hydroxyapatite cement in moderate stress-bearing bone repairs. In addition, the cyclic fatigue properties of the CPC<sub>D</sub>-fiber composite also need to be investigated to simulate the cyclic loading in clinical applications.

In a previous study on fiber reinforcement of CPC, a semiempirical equation was obtained that relates the CPC-fiber composite strength,  $S_c$ , to the fiber strength,  $S_f$ <sup>28</sup>

$$S_c = S_m + \alpha S_f \quad (1)$$

where  $S_m$  is the strength of the matrix, and  $\alpha$  is a coefficient. Fitting the experimental data to Eq. (1) yielded  $S_c = 12.5 + 0.0082S_f$  for the compositions used in the previous study.<sup>28</sup> In that study, the matrix was held constant, and  $S_f$  was varied by using different types of fibers.<sup>28</sup> In the present study,  $S_f$  was kept constant, and the CPC matrix was varied by changing the incubation time. The coefficient  $\alpha$  in Eq. (1) should be proportional to  $S_m$ , because when the CPC paste did not set,  $S_m = 0$  and  $S_c = 0$ , thus requiring that  $\alpha = 0$ . This is because there was no matrix holding and supporting the fibers. Although the fibers are strong, without a matrix there is no composite nor composite strength. Hence it is assumed that  $\alpha = \beta S_m$  to satisfy the condition that in Eq. (1), when  $S_m = 0$ , so should  $S_c$ , even when  $S_f$  is not zero. Therefore,  $S_c = S_m + \beta S_m S_f = S_m (1 + \beta S_f)$ , and finally

$$S_c = \gamma S_m \quad (2)$$

where  $\gamma = 1 + \beta S_f$ . Figure 7 plots the measured composite strength  $S_c$  from Figure 6 versus the corresponding  $S_m$  from Figure 2. The straight line in Figure 7 is a linear best fit through the origin with a correlation coefficient  $R = 0.93$ , yielding

$$S_c = 2.16 S_m \quad (3)$$

This suggests that

1. When the fiber type, fiber length, and fiber volume fraction were kept constant, the composite



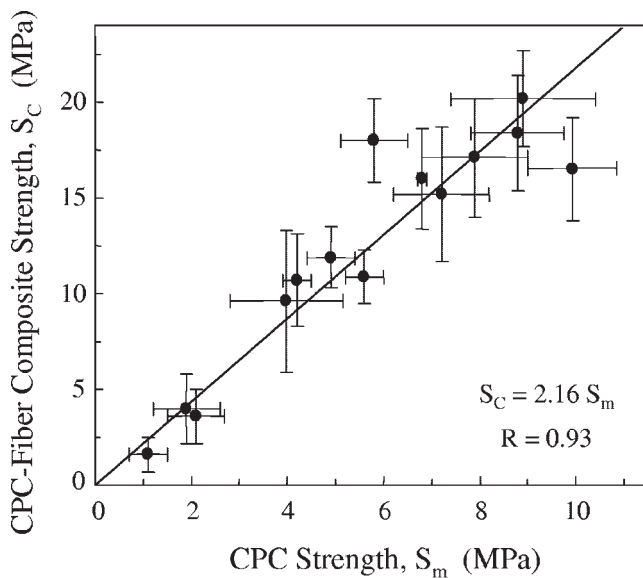


**Figure 7.** Experimentally measured data on composite strength,  $S_c$ , and CPC matrix strength,  $S_m$ , were fitted to Eq. (2) by linear regression, resulting in the establishment of Eq. (3):  $S_c = 2.16S_m$ , with a correlation coefficient  $R = 0.93$ . Each value was the mean of five measurements, with the error bar showing one standard deviation (mean  $\pm$  SD;  $n = 5$ ).

strength increased linearly when the matrix strength was increased.

2. The CPC composite strength was, in general, 2.16 times higher than the strength of CPC without fibers, when the suture fibers at 25% volume fraction and 8-mm length were randomly mixed into the CPC paste.

Although this study focused on the development of early strength for the implant, previous studies investigated the longer-term properties of absorbable fiber-reinforced CPC.<sup>14,24,41</sup> The suture fibers were chosen because a previous clinical study showed that these fibers had significant potential as an absorbable dural substitute with minimal inflammatory reaction.<sup>42</sup> These large-diameter fibers provided significant strength and toughness to the implant for several weeks.<sup>24</sup> Then, long cylindrical macropores of  $293 \pm 46 \mu\text{m}$  in diameter were created in CPC after fiber dissolution.<sup>24,43</sup> When implanted *in vivo*, the fibers should degrade to expose macropores for bony ingrowth. The strengthening of the graft from bony ingrowth and the deposition of new bone<sup>34,44</sup> should help offset the weakening of the graft due to fiber degradation. The CPC-fiber composite was shown in a previous study to support osteoblast cell adhesion, proliferation, and viability.<sup>43</sup> The method of using large-diameter absorbable fibers in bone graft for mechanical strengthening and formation of long cylindrical macropores for bone ingrowth may be applicable to other tissue-engineering materials.

## SUMMARY

Substantial early strength and toughness were imparted to a moldable, self-hardening, and resorbable hydroxyapatite bone repair material via two approaches: the use of DCPD instead of DCPA, and the incorporation of absorbable fibers. As a result, the paste hardening time was reduced from about 80 min to 15 min, which should significantly shorten the surgical time. SEM revealed the progressive formation of nanosized rod-like hydroxyapatite crystals and platelet crystals in the cements. The flexural strength quickly reached 10.7 MPa for the CPC<sub>D</sub>-fiber cement in 30 min, compared to 0 MPa for the conventional CPC<sub>A</sub>, which did not set. Such a high early strength matched the reported strength for cancellous bone and sintered porous hydroxyapatite implants. The work of fracture (toughness) was increased by two orders of magnitude for CPC<sub>D</sub>-fiber specimens. A previous study observed disintegration of the conventional CPC implant, "possibly due to lower initial mechanical strength, resulting in severe foreign-body response."<sup>4</sup> Therefore, the high early strength and toughness of the new CPC<sub>D</sub>-fiber formulation, developed in the present study, should help protect the implant from catastrophic fracture or disintegration under stresses. The composite strength was correlated to the matrix strength by  $S_c = 2.16S_m$ , suggesting that the development of a strong matrix was as important as the incorporation of a strong reinforcing agent. The method of synergistic use of a strong matrix (CPC<sub>D</sub>) and a reinforcing agent (absorbable fibers) in a bone graft may be applicable to other tissue-engineering materials.

The authors thank Dr. F. C. Eichmiller and Dr. S. H. Dickens for discussions, and A. A. Giuseppetti for experimental assistance.

## References

1. Brown WE, Chow LC. A new calcium phosphate water setting cement. In: Brown PW, editor. Cements research progress. Westerville, OH: American Ceramic Society; 1986. p 352–379.
2. Ginebra MP, Fernandez E, De Maeyer EAP, Verbeeck RMH, Boltong MG, Ginebra J, Driessens FCM, Planell JA. Setting reaction and hardening of an apatite calcium phosphate cement. *J Dent Res* 1997;76:905–912.
3. Knaack D, Goad MEP, Aiolo M, Rey C, Tofighi A, Chakravarthy P, Lee DD. Resorbable calcium phosphate bone substitute. *J Biomed Mater Res Appl Biomater* 1998;43:399–409.
4. Miyamoto Y, Ishikawa K, Takechi M, Toh T, Yuasa T, Nagayama M, Suzuki K. Histological and compositional evaluations of three types of calcium phosphate cements when implanted in subcutaneous tissue immediately after mixing. *J Biomed Mater Res Appl Biomater* 1999;48:36–42.
5. Barralet JE, Gaunt T, Wright AJ, Gibson IR, Knowles JC. Effect of porosity reduction by compaction on compressive strength

- and microstructure of calcium phosphate cement. *J Biomed Mater Res (Appl Biomater)* 2002;63:1–9.
6. Yokoyama A, Yamamoto S, Kawasaki T, Kohgo T, Nakasu M. Development of calcium phosphate cement using chitosan and citric acid for bone substitute materials. *Biomaterials* 2002;23:1091–1101.
  7. Friedman CD, Costantino PD, Jones K, Chow LC, Pelzer HJ, Sisson GA. Hydroxyapatite cement: II, Obliteration and reconstruction of the cat frontal sinus. *Arch Otolaryngol Head Neck Surg* 1991;117:385–389.
  8. Costantino PD, Friedman CD, Jones K, Chow LC, Sisson GA. Experimental hydroxyapatite cement cranioplasty. *Plast Reconstr Surg* 1992;90:174–191.
  9. Shindo ML, Costantino PD, Friedman CD, Chow LC. Facial skeletal augmentation using hydroxyapatite cement. *Arch Otolaryngol Head Neck Surg* 1993;119:185–190.
  10. Friedman CD, Costantino PD, Takagi S, Chow LC. BoneSource hydroxyapatite cement: a novel biomaterial for craniofacial skeletal tissue engineering and reconstruction. *J Biomed Mater Res (Appl Biomater)* 1998;43:428–432.
  11. Chow LC. Calcium phosphate cements: Chemistry, properties, and applications. *Mater Res Symp Proc* 2000;599:27–37.
  12. Brown GD, Mealey BL, Nummikoski PV, Bifano SL, Waldrop TC. Hydroxyapatite cement implant for regeneration of periodontal osseous defects in humans. *J Periodontol* 1998;69:146–157.
  13. Ueyama Y, Ishikawa K, Mano T, Koyama T, Nagatsuka H, Matsumura T, Suzuki K. Initial tissue response to anti-washout apatite cement in the rat palatal region: Comparison with conventional apatite cement. *J Biomed Mater Res* 2001;55:652–660.
  14. Xu HHK, Takagi S, Quinn JB, Chow LC. Fast-setting calcium phosphate scaffolds with tailored macropore formation rates for bone regeneration. *J Biomed Mater Res A* 2004;68:725–734.
  15. Cherng A, Takagi S, Chow LC. Effects of hydroxypropyl methylcellulose and other gelling agents on the handling properties of calcium phosphate cement. *J Biomed Mater Res* 1997;35:273–277.
  16. Takagi S, Chow LC, Hirayama S, Eichmiller FC. Properties of elastomeric calcium phosphate cement–chitosan composites. *Dent Mater* 2003;19:797–804.
  17. Xu HHK, Quinn JB, Takagi S, Chow LC. Processing and properties of strong and non-rigid calcium phosphate cement. *J Dent Res* 2002;81:219–224.
  18. Burguera EF, Guitian F, Chow LC. A water setting tetracalcium phosphate—dicalcium phosphate dihydrate cement. *J Biomed Mater Res A* 2004;71A:275–282.
  19. Chow LC. Solubility of calcium phosphates. In: Chow LC, Eanes ED, editors. *Octacalcium phosphate*. Basel, Switzerland: Karger, 2001. p 94–111.
  20. Chow LC, Markovic M, Takagi S. A dual constant-composition titration system as an *in vitro* resorption model for comparing dissolution rates of calcium phosphate biomaterials. *J Biomed Mater Res B* 2003;65B:245–251.
  21. Takagi S, Chow LC, Hirayama S, Sugawara A. Premixed calcium phosphate cement pastes. *J Biomed Mater Res B* 2003;67B:689–696.
  22. ADA specification no. 9 for dental silicate cement. *Guide to dental materials and devices*. 7<sup>th</sup> edition. Chicago, IL: American Dental Association; 1974/1975. p 194–202.
  23. Fukase Y, Eanes ED, Takagi S, Chow LC, Brown WE. Setting reactions and compressive strengths of calcium phosphate cement. *J Dent Res* 1990;69:1852–1856.
  24. Xu HHK, Quinn JB. Calcium phosphate cement containing resorbable fibers for short-term reinforcement and macroporosity. *Biomaterials* 2002;23:193–202.
  25. Xu HHK, Quinn JB, Takagi S, Chow LC, Eichmiller FC. Strong and macroporous calcium phosphate cement: Effects of porosity and fiber reinforcement on mechanical properties. *J Biomed Mater Res* 2001;57:457–466.
  26. Ishikawa K, Miyamoto Y, Takechi M, Toh T, Kon M, Nagayama M, Asaoka K. Non-decay type fast-setting calcium phosphate cement: Hydroxyapatite putty containing an increased amount of sodium alginate. *J Biomed Mater Res* 1997;36:393–399.
  27. Costantino PD, Friedman CD, Jones K, Chow LC, Pelzer HJ, Sisson GA. Hydroxyapatite cement. *Arch Otolaryngol Head Neck Surg* 1991;117:379–384.
  28. Xu HHK, Eichmiller FC, Giuseppetti AA. Reinforcement of a self-setting calcium phosphate cement with different fibers. *J Biomed Mater Res* 2000;52:107–114.
  29. Komath M, Varma HK, Sivakumar R. On the development of an apatitic calcium phosphate bone cement. *Bull Mater Sci* 2000;23:135–140.
  30. Otsuka M, Matsuda Y, Suwa Y, Fox JL, Higuchi WI. Effect of particle size of metastable calcium phosphates on mechanical strength of a novel self-setting bioactive calcium phosphate cement. *J Biomed Mater Res* 1995;29:25–32.
  31. Hamanishi C, Kitamoto K, Tanaka S, Otsuka M, Doi Y, Kitahashi T. A self-setting TTCP-DCPD apatite cement for release of vancomycin. *J Biomed Mater Res* 1996;33:139–143.
  32. Komath M, Varma HK. Development of a fully injectable calcium phosphate cement for orthopedic and dental applications. *Bull Mater Sci* 2003;26:415–422.
  33. Chow LC, Markovic M, Takagi S, Cherng A. Effects of cement liquid on the physical properties of the cement. *Innov Technol Biol Med* 1997;18:11–14.
  34. Suchanek W, Yoshimura M. Processing and properties of hydroxyapatite-based biomaterials for use as hard tissue replacement implants. *J Mater Res* 1998;13:94–117.
  35. Damien CJ, Parsons JR. Bone graft and bone graft substitutes: A review of current technology and applications. *J Appl Biomater* 1991;2:187–208.
  36. Mellonig JT. Freeze-dried bone allografts in periodontal reconstructive surgery. *Dent Clin North Am* 1991;35:505–520.
  37. Garrett JS. Periodontal regeneration around natural teeth. *Ann Periodontol* 1996;1:621–666.
  38. Broz JJ, Simske SJ, Corley WD, Greenberg AR. Effects of deproteinization and ashing on site-specific properties of cortical bone. *J Mater Sci Mater Med* 1997;8:395–401.
  39. O'Kelly K, Tancred D, McCormack B, Carr A. A quantitative technique for comparing synthetic porous hydroxyapatite structure and cancellous bone. *J Mater Sci Mater Med* 1996;7:207–213.
  40. Lucksanasonboon P, Higgs WAJ, Higgs RJED, Swain MV. Fracture toughness of bovine bone: influence of orientation and storage media. *Biomaterials* 2001;22:3127–3132.
  41. Xu HHK, Quinn JB, Takagi S, Chow LC. Synergistic reinforcement of *in situ* hardening calcium phosphate composite scaffold for bone tissue engineering. *Biomaterials* 2004;25:1029–1037.
  42. Maurer PK, McDonald JV. Vicryl (polyglactin 910) mesh as a dural substitute. *J Neurosurg* 1985;63:448–452.
  43. Xu HHK, Simon CG Jr. Self-hardening calcium phosphate composite scaffold for bone tissue engineering. *J Orthop Res* 2004;22:535–543.
  44. Tamai N, Myoui A, Tomita T, Nakase T, Tanaka J, Ochi T, Yoshikawa H. Novel hydroxyapatite ceramics with an interconnective porous structure exhibit superior osteoconduction *in vivo*. *J Biomed Mater Res* 2002;59:110–117.